

# Single Cell-Based Vector Tracing in Patients with ADA-SCID Treated with Stem Cell Gene Therapy

Yuka Igarashi,<sup>1</sup> Toru Uchiyama,<sup>1</sup> Tomoko Minegishi,<sup>1</sup> Sirirat Takahashi,<sup>1</sup> Nobuyuki Watanabe,<sup>1</sup> Toshinao Kawai,<sup>1</sup> Masafumi Yamada,<sup>2</sup> Tadashi Ariga,<sup>2</sup> and Masafumi Onodera<sup>1</sup>

<sup>1</sup>Department of Human Genetics, National Center for Child Health and Development, Tokyo 157-8535, Japan; <sup>2</sup>Department of Pediatrics, Hokkaido University Graduate School of Medicine, Hokkaido 060-8638, Japan

**Clinical improvement in stem cell gene therapy (SCGT) for primary immunodeficiencies depends on the engraftment levels of genetically corrected cells, and tracing the transgene in each hematopoietic lineage is therefore extremely important in evaluating the efficacy of SCGT. We established a single cell-based droplet digital PCR (sc-ddPCR) method consisting of the encapsulation of a single cell into each droplet, followed by emulsion PCR with primers and probes specific for the transgene. A fluorescent signal in a droplet indicates the presence of a single cell carrying the target gene in its genome, and this system can clearly determine the ratio of transgene-positive cells in the entire population at the genomic level. Using sc-ddPCR, we analyzed the engraftment of vector-transduced cells in two patients with severe combined immunodeficiency (SCID) who were treated with SCGT. Sufficient engraftment of the transduced cells was limited to the T cell lineage in peripheral blood (PB), and a small percentage of CD34<sup>+</sup> cells exhibited vector integration in bone marrow, indicating that the transgene-positive cells in PB might have differentiated from a small population of stem cells or lineage-restricted precursor cells. sc-ddPCR is a simplified and powerful tool for the detailed assessment of transgene-positive cell distribution in patients treated with SCGT.**

## INTRODUCTION

Stem cell-based gene therapy has been proposed as a highly desirable treatment for primary immunodeficiencies (PIDs) when patients lack human leukocyte antigen (HLA)-matched suitable donors for hematopoietic stem cell transplantation (HSCT). The addition of the therapeutic gene to autologous hematopoietic stem cells (HSCs) is an attractive alternative because the gene-corrected HSCs are expected to reconstitute the functional immune system in the same manner as allogeneic HSCs in treated patients.<sup>1-4</sup> A series of HSC-based gene therapy clinical trials confirmed this expectation, revealing that treated patients displayed multi-lineage expression of the transduced gene.<sup>5-12</sup>

To achieve clinical improvement, sufficient engraftment of the transduced cells is required, although various factors, including the selec-

tive advantage of the therapeutic gene, affect their engraftment in bone marrow (BM).<sup>5,6,10-12</sup> Therefore, the mapping of gene-transduced cell distributions in treated patients is required to evaluate the efficacy of gene therapy. Recently, advances in the genetic characterization of a single cell provided insights into genomic and transcriptomic heterogeneity,<sup>13</sup> and such insights can be helpful in the field of gene therapy.

In this study, we developed a single cell-based droplet digital PCR (sc-ddPCR) system consisting of single-cell encapsulation, droplet PCR using a fluorescent probe, and the detection of signal-positive droplets. This novel strategy enables direct detection of the vector sequence at the genomic level in each cell of the target population. Using the established method, we analyzed gene therapy-treated patients with adenosine deaminase (ADA)-deficient severe combined immunodeficiency (SCID), which is caused by mutation of the ADA gene. ADA is important for the purine metabolic pathway, and genetic defects in the ADA gene result in autosomal recessive type SCID.<sup>14</sup> For patients without suitable HSCT donors, enzyme replacement therapy with polyethylene glycol-modified bovine ADA (PEG-ADA) is a widely used treatment option worldwide.<sup>15</sup> However, PEG-ADA therapy often results in partial immune reconstitution,<sup>16</sup> and gene therapy using autologous HSCs has been studied as an alternative curative treatment for those patients.<sup>6</sup>

In current gene therapy approaches for ADA deficiency, withdrawal of PEG-ADA and preconditioning treatment with busulfan are indispensable for achieving full engraftment of gene-transduced cells in all hematopoietic lineages.<sup>6,9,17</sup> In 2015, we reported two patients with ADA-SCID who were treated with retrovirus-mediated gene therapy.<sup>18</sup> Although PEG-ADA replacement was withdrawn in our trial, the patients never received preconditioning chemotherapy before the

Received 4 April 2016; accepted 18 May 2017;  
<http://dx.doi.org/10.1016/j.omtm.2017.05.005>.

**Correspondence:** Toru Uchiyama, MD, PhD, Department of Human Genetics, National Center for Child Health and Development, 2-10-1, Okura, Setagaya-ku, Tokyo 157-8535, Japan.

**E-mail:** [uchiyama-t@ncchd.go.jp](mailto:uchiyama-t@ncchd.go.jp)

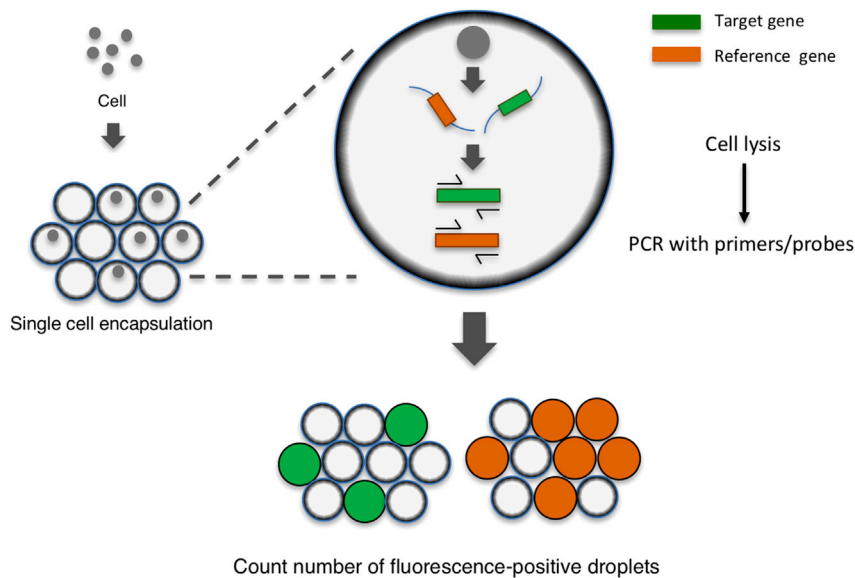


**Figure 1. Schematic of the Single Cell-Based Digital Droplet PCR System**

Cells from the target population were encapsulated into droplets at a concentration of one cell/droplet with the PCR mixture including primers and probes. After single-cell encapsulation, cell lysis and amplification of the target sequence were performed within the droplets. The number of droplets with a fluorescent signal indicates the number of cells carrying the target or reference gene. sc-ddPCR, single cell-based digital droplet PCR.

PCR using a standard composition of solution mix and a standard program did not produce any signals in the droplets, which indicated the failure of cell lysis inside the droplet (Figure 2D, upper panels). Therefore, we added additional SDS to the reaction, and as part of the cell lysis step, we incorporated preheating at 85°C into the PCR program. To amplify

the target gene in the presence of undesirable substances such as inhibitors from lysed cells, we further added DNA polymerase to the reaction (Tables S1 and S2). After these modifications, clear fluorescent signals were observed in the droplets (Figure 2D, lower panels), and this high fluorescent amplitude of vector  $\psi$  and *RPP30* was sufficient to permit separation from that of negative samples. The fluorescent signal in each droplet directly indicated the existence of a cell carrying the vector inside the droplet.

transplantation of gene-modified HSCs; therefore, partial and temporal reconstitution of the immune system was observed in both patients.

Our sc-ddPCR method allowed us to assess the detailed distribution of the vector-containing cells in peripheral blood (PB) and BM and revealed the skewed engraftment of gene-transduced cells in the hematopoietic systems of these patients.

## RESULTS

### Single-Cell Encapsulation into a Droplet

The sc-ddPCR system commenced with the encapsulation of a single cell into one droplet and then proceeded to the step of PCR using a TaqMan hydrolysis probe, followed by detection of the fluorescent signal in the droplets (Figure 1). K562 cells were transduced with a retroviral vector expressing ADA and EGFP (Figure 2A). Cell clones with single copy integration, which enabled us to trace vector integration via EGFP expression, were used for the following experiments (K562-AE cells).

We added various numbers of K562-AE cells to the standard PCR reaction directly and generated droplets using the QX200 system's droplet generator. The 2,000-cell samples were successfully encapsulated into droplets, and single-cell encapsulation was observed in 98% of the cell-containing droplets (Figures 2B and 2C). However, samples containing more than 8,000 cells displayed multi-cell encapsulation, and several cells were located outside the droplets. We also confirmed that single-cell encapsulation is not influenced by cell type, based on the result of 2,000-cell encapsulation using PB mononuclear cells (PBMCs) and cord blood mononuclear cells (Figure S1).

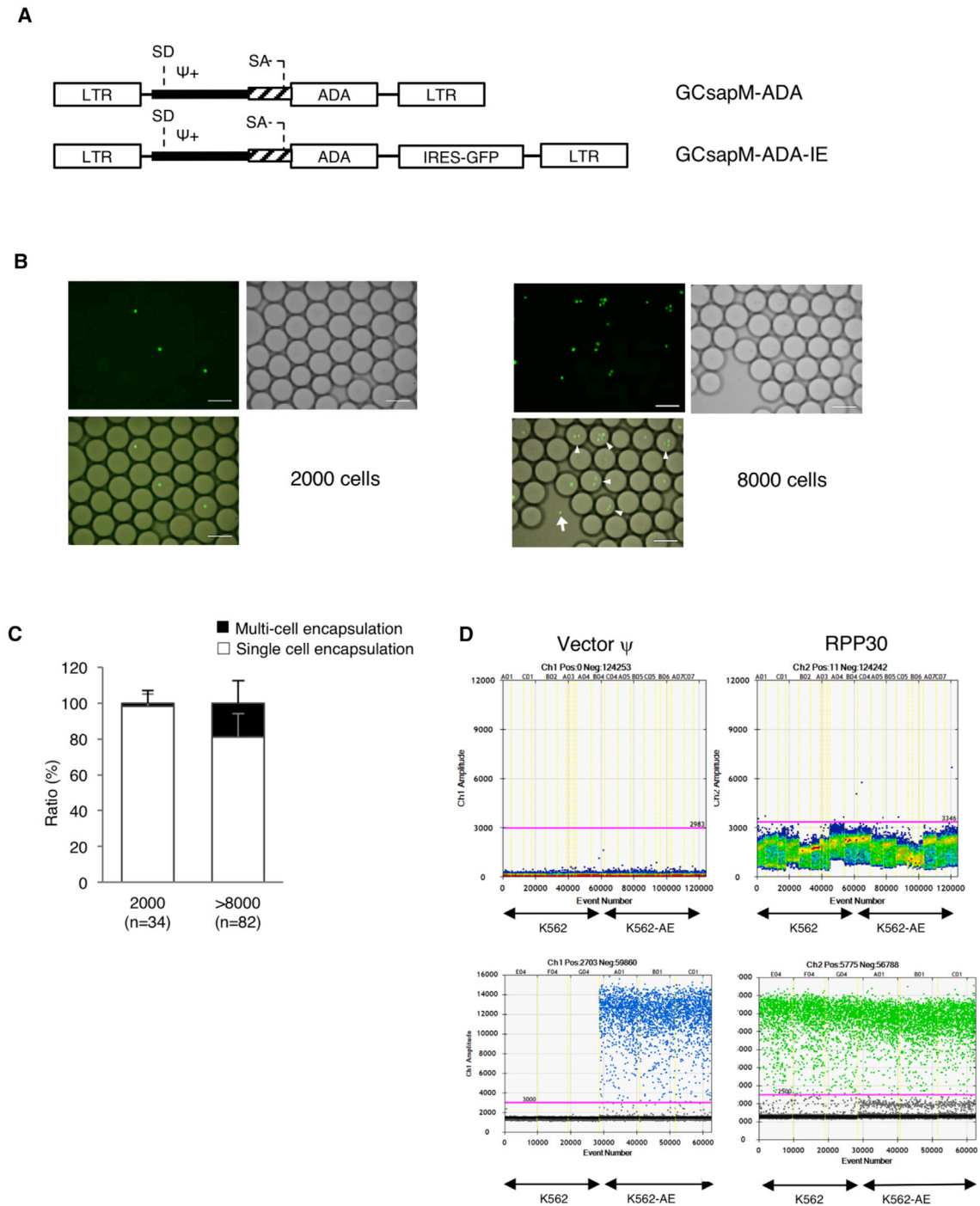
### Direct PCR Inside Droplets

Direct PCR subsequent to cell encapsulation requires cell lysis within each droplet to amplify the target sequence in the genome.

### Assessment of the Detection Capability of sc-ddPCR

We first estimated the accuracy of the sc-ddPCR system's detection capability using K562-AE cells. Non-specific vector signals in negative samples could lead to overestimation of the frequency of vector-positive cells. An extremely low vector signal could be observed in non-transduced K562 cells (vector  $\psi$ /*RPP30* = 0.0006) as well as PBMCs and cord blood CD34<sup>+</sup> cells (vector  $\psi$ /*RPP30* = 0.00036 and 0.00042, respectively) (Figure 3A). We concluded that the level of false positivity due to non-specific vector signals was minimal. Multi-cell encapsulation may decrease the number of signal-positive droplets because, for example, two to three cells encapsulated in one droplet are calculated as "one cell" in sc-ddPCR. To evaluate the influence of multi-cell encapsulation, we analyzed 10,000- or 20,000-cell samples by encapsulating the cells in one reaction or dividing the cells into reactions with 2,000 cells each. Encapsulation of the cells into one reaction resulted in a lower number of signals due to multi-cell encapsulation (Figure S2), which revealed the importance of single-cell encapsulation for accurate evaluation.

We then examined whether sc-ddPCR could clarify the ratios of target cells among the populations. Naive K562 cells were spiked with one-copy K562-AE cells at serially diluted ratios. Using genomic DNA extracted from each sample, we analyzed the levels of the vector  $\psi$  sequence and internal reference gene *RPP30* using



(A) The structure of the retroviral vector used in this study. GCsapM-ADA was used in the clinical trials. EGFP cDNA was incorporated downstream of ADA cDNA with the sequence of an internal ribosomal entry site (IRES) in the pGCsapM-ADA-IE construct. K562 cells were transduced with GCsapM-ADA-IE to create K562-AE cells. (B) Direct encapsulation of K562-AE cells into droplets. The 2,000-cell samples exhibited single-cell encapsulation into droplets. Multi-cell encapsulation (triangles) and the failure of encapsulation (arrows) were observed in samples containing more than 8,000 cells. Fluorescent (EGFP) and bright-field (BF) images are shown. Scale bars represent 100  $\mu$ m. (C) Ratios of droplets with single- or multi-cell encapsulation. Droplets were counted in 34 and 82 different fields on microscopy in the 2,000- and > 8,000-cell samples, respectively. (D) Direct PCR subsequent to single-cell encapsulation. Droplets containing a single cell displayed fluorescent signals after amplification of the vector  $\psi$  and reference gene *RPP30*. Upper panels, standard procedure; lower panels, modified procedure. LTR, long terminal repeat; SA, splice acceptor; SD, splice donor.

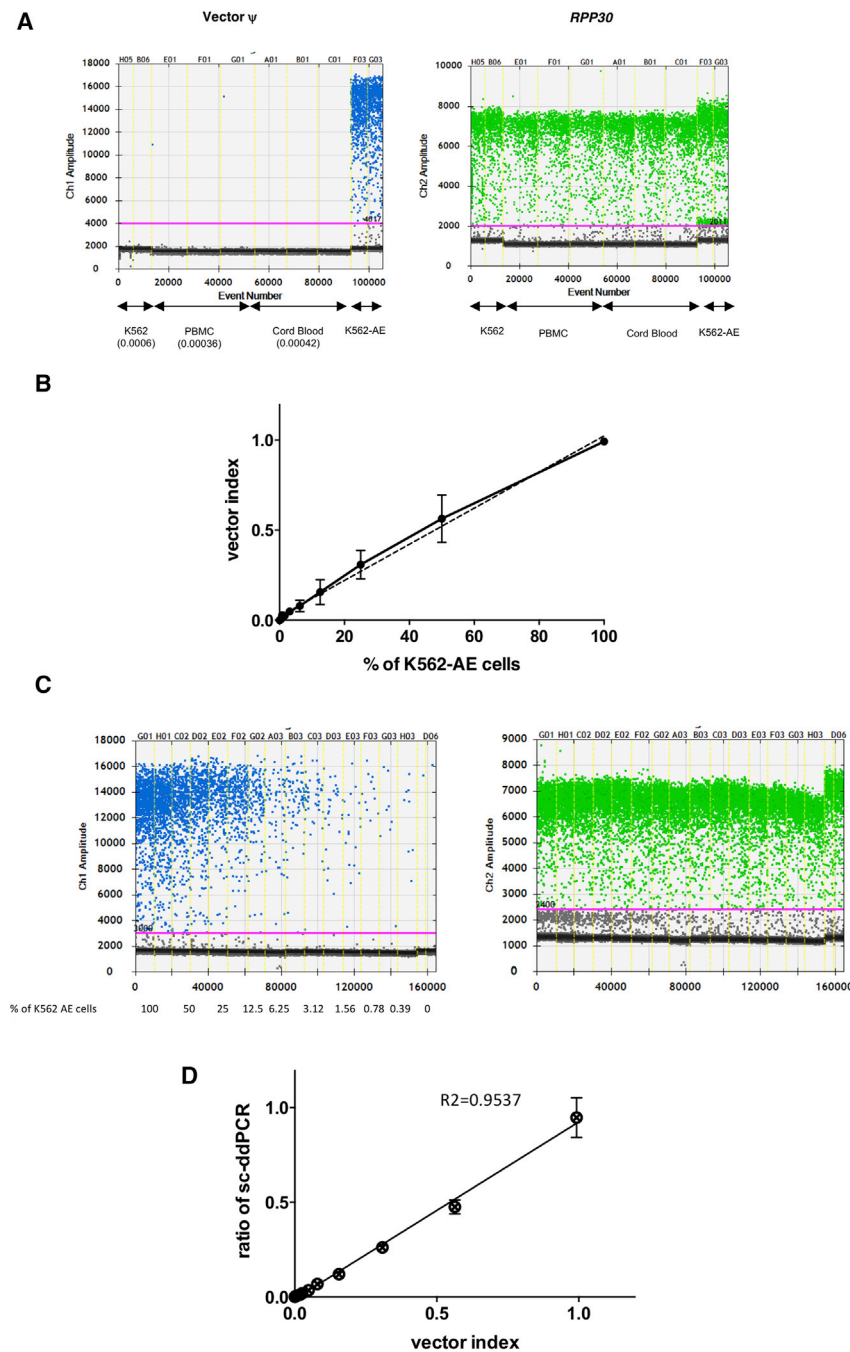


**Figure 3. Estimation of the Accuracy of Single Cell-Based Digital Droplet PCR**

(A) Evaluation of the non-specific signals in negative samples. Target  $\psi$  and *RPP30* were amplified in mononuclear cell samples of peripheral blood (PBMCs) and cord blood from healthy donors, as well as naive K562 cells. The ratio of the target  $\psi$ , which denotes the background signal, is shown below each sample. (B) Relationship between the percentages of dilution and the vector index in extracted genomic DNA from spiked cell samples. K562 cell samples were spiked with serially diluted K562-AE cells carrying the vector at a concentration of one copy per cell. Vector  $\psi$  and *RPP30* were measured using genomic DNA from spiked samples by conventional ddPCR. The vector index was calculated using the following formula:  $(2 \times \text{number of vector-positive droplets}) / (\text{numbers of } RPP30\text{-positive droplets})$ . An index of 1 indicates that all cells contain one copy of  $\psi$  and two copies of *RPP30* in their genomes. The measured value in each spiked sample was linearly related to the theoretical values. (C) Single cell-based digital droplet PCR (sc-ddPCR) using spiked samples. K562 cell samples spiked with serially diluted K562-AE cells were analyzed by sc-ddPCR. The number of  $\psi$  signal-positive droplets, which contain vector-positive cells, declined in relationship with the spiked ratios, whereas similar numbers of *RPP30*-positive droplets were observed irrespective of the spiked ratio, which indicated the sample size. (D) Correlation between the vector index and the ratio of vector-positive droplets as determined by sc-ddPCR. sc-ddPCR was performed using spiked K562 cells, and the measured values were plotted against the vector index in genomic DNA. The ratios determined by sc-ddPCR were linearly related to the vector index.

ure 3C). The ratio of vector-positive cells was calculated as follows: vector-positive ratio = (number of vector-positive droplets)/(number of *RPP30*-positive droplets). The signal for *RPP30* denotes the sample size; therefore, the droplet numbers were always constant among the spiked samples. Meanwhile, the ratio of droplets positive for vector  $\psi$  deteriorated consistent with the pre-designed proportion of K562-AE cells in each sample (Figure 3C). In each spiked sample, the ratio of vector-positive cells according to sc-ddPCR significantly corresponded to the vector index in extracted genomic DNA at levels  $\geq 0.004$  (Figure 3D;

the ddPCR system and calculated the vector index as described in the Materials and Methods. The determined index indicated the actual ratios of the serial dilution at the genomic level in the spiked cell samples (Figure 3B). These spiked samples were then enclosed into droplets at 2,000 cells per reaction, and sc-ddPCR was performed with the modified protocol for detecting vector  $\psi$  and *RPP30*. The fluorescent signal in each droplet indicated the presence of a cell containing the target sequence in its genome (Fig-

Table 1). These data revealed that sc-ddPCR enabled direct detection of the provirus sequence in cells without DNA extraction.

#### sc-ddPCR Revealed Skewed Engraftment of Hematopoietic Lineages in Gene Therapy-Treated Patients

Using this novel system, we then analyzed two patients with ADA-SCID treated with stem cell gene therapy (SCGT) using the retroviral vector GCsapM-ADA in 2003 and 2004, respectively. Patient

**Table 1. Comparison of the Vector Index of Genomic DNA and Ratios of Vector-Positive Cells**

Vector Index on gDNA <sup>a</sup>	Ratio of sc-ddPCR
0.992	0.954
0.564	0.475
0.304	0.261
0.156	0.12
0.079	0.068
0.049	0.035
0.026	0.018
0.017	0.018
0.004	0.004
0	0.0006

gDNA, genomic DNA.

<sup>a</sup>The vector index was calculated with the following formula using extracted genomic DNA:  $(2 \times \text{number of vector-positive droplets}) / (\text{number of RPP30-positive droplets})$ .

characterization and a summary of the treatment were previously reported. Briefly, administration of PEG-ADA for both patients was discontinued 5 weeks prior to harvesting BM. The doses of CD34<sup>+</sup> cells administered were  $1.38 \times 10^6$  cells/kg for patient 1 (Pt1) and  $0.92 \times 10^6$  cells/kg for patient 2 (Pt2), with transduction efficiencies of approximately 40% and 50%, respectively. Neither patient previously received cytoreductive treatments such as busulfan before the manipulated cells were infused; therefore, they experienced partial improvements in immune system function, in addition to improvements of their clinical courses. The current immunological and hematological characterization of the patients is shown in Figure 4A. Although the existence of three lymphocyte lineages (CD3<sup>+</sup> T cells, CD19<sup>+</sup> B cells, and CD56<sup>+</sup> natural killer [NK] cells) in PB was observed in Pt1, the B lymphocyte lineage was markedly reduced in Pt2. In BM, the proportions of CD34<sup>+</sup> subset that contained hematopoietic repopulating cells were 6.8% (Pt1) and 1.7% (Pt2). Detailed information about the number of lymphocytes in PB and nucleated cells in BM are described in the Supplemental Information.

sc-ddPCR analysis was then performed for both patients. PBMCs corrected from patients were sorted into CD3<sup>+</sup> T cell, CD56<sup>+</sup> NK cell, and CD19<sup>+</sup> B cell subsets by fluorescence-activated cell sorting (FACS) and then enclosed in the droplets. In sc-ddPCR analysis, almost all of the existing CD3<sup>+</sup> T cells exhibited vector integration in the genome (97.1% in Pt1 and 80.8% in Pt2), whereas only some CD56<sup>+</sup> NK and CD19<sup>+</sup> B cells displayed vector integration (Figure 4B). The possibility of false positivity in B and NK cells due to the contamination of T cells was eliminated by checking the purity of the sorted cells (Figure S3). These results indicated that ADA-positive T cells have a strong growth advantage over non-transduced cells. In the BM of Pt1, the entire nucleated cell population and a fraction of CD34<sup>+</sup> cells exhibited extremely low levels of vector integration (Figure 4C). Pt1 displayed vector integration in 4.5% of all nucleated cells and 1.73% of CD34<sup>+</sup> cells. Although Pt2 had a higher

ratio of vector integration in all nucleated cells (6.6%), the patient's CD34<sup>+</sup> cells displayed no vector integration. Based on these results, both patients displayed long-standing engraftment of gene-transduced HSCs in BM at a remarkably low level.

#### Calculation of Vector Copy Numbers in the Population of Gene-Transduced Cells

We also determined the vector copy number (VCN) restricted to the fraction of transduced cells (tVCN) of the target population based on the ratio of vector-positive cells by sc-ddPCR and the average copy number in genomic DNA (aVCN) via conventional ddPCR, as described in the Materials and Methods. For the preliminary experiment using cell lines, we also prepared K562 cell clones with various numbers of copies (one, two, four, and five) of the vector sequence. K562 cell samples serially diluted with these cells were assayed regarding the ratio of vector-positive cells and the aVCN by sc-ddPCR and conventional ddPCR, respectively. In most spiked samples, the copy number was almost correctly calculated on the basis of these measured values in accordance with the pre-determined actual copy numbers (Table S4).

Using this method, we measured the tVCNs in the sorted fractions from PBMCs and BM. Interestingly, in the PBMC samples, whereas T cells displayed the integration of approximately one copy, more integrated vectors were detected in the vector-positive fractions from B and NK cells (Figure 5; Table 2). These results revealed that lower numbers of integrated vectors could provide a selective advantage to T cells, whereas B and NK cells, even with greater vector integration, could not expand predominantly over the non-transduced cells.

#### DISCUSSION

In hematopoietic SCGT, nonmyeloablative conditioning with busulfan has been performed to secure the BM niche for gene-transduced cells since a report by Aiuti et al.<sup>6,17,19</sup> By contrast, our patients did not receive preconditioning therapy, and they exhibited partial and temporal immune reconstitution.<sup>18</sup> We also reported that one of the patients later began to display gastrointestinal distress and failure to thrive, likely caused by incomplete immune recovery.<sup>20</sup> Genetic and cytological analysis of the engraftment of gene-transduced cells was therefore imperative for evaluating the efficacy of treatment and assessing the influence of the protocol on their engraftment, but this was extremely difficult using conventional approaches.

Determining transduction efficiency at the genomic level has commonly been performed by PCR using genomic DNA samples after whole-genome amplification from a single cell<sup>13</sup> or colony-PCR using DNA from colony-forming cells.<sup>21,22</sup> Although qPCR is effective for analyzing patients' genetic characteristics after gene therapy, there are some technical difficulties associated with a single-cell assay. A novel technology, ddPCR, was recently developed to enable the absolute quantification of nucleic acid target sequences. PCR with a TaqMan probe is performed within each droplet containing fragmented DNA, and the presence of the target gene is determined by counting the number of fluorescent signal-positive droplets.<sup>23–25</sup>

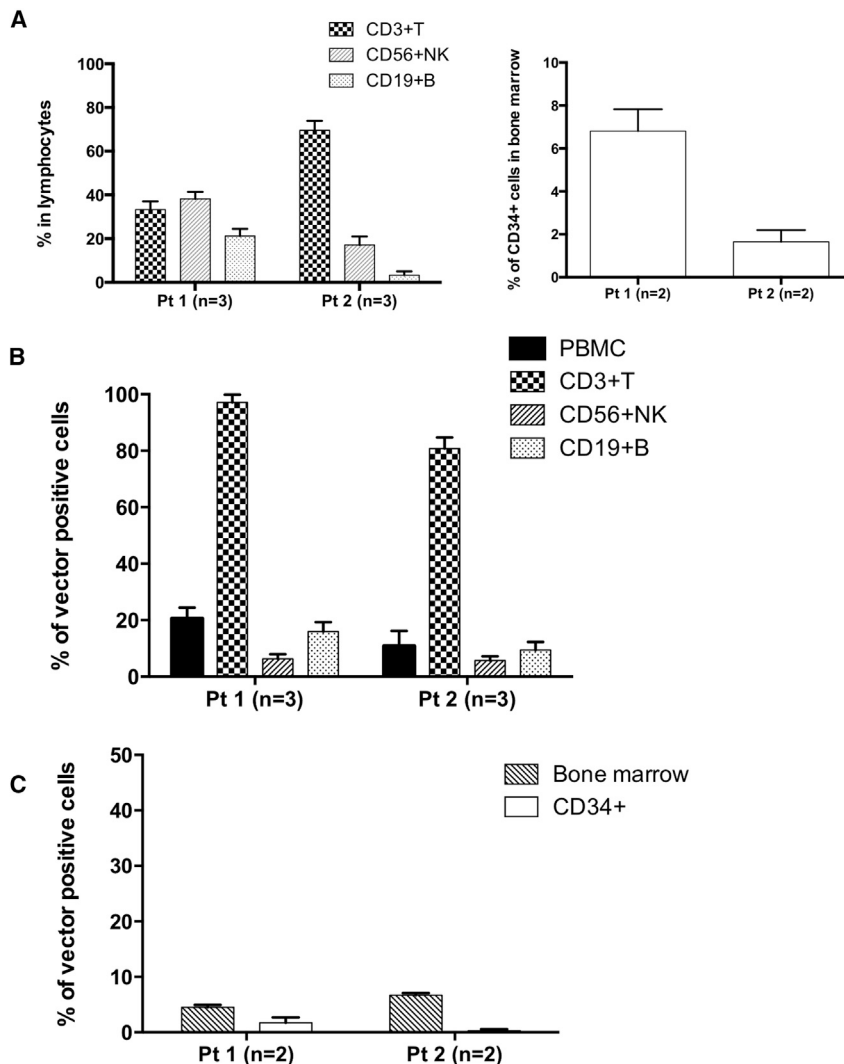


**Figure 4. Droplet-Based Single-Cell PCR Analysis of Peripheral Blood and Bone Marrow Samples from Patients**

Droplet-based single-cell PCR (dsPCR) was performed using samples from two patients. (A) Immunological characterization of peripheral blood and bone marrow samples from patients via FACS analysis. Percentages of CD3<sup>+</sup> T cells, CD56<sup>+</sup> NK cells, and CD19<sup>+</sup> B cells in lymphocytes are shown in the bar chart. Bone marrow samples were also analyzed for CD34 expression. (B) Ratios of vector-positive cells in the whole PBMC and sorted fractions. PBMC samples from patients were sorted via FACS into CD3<sup>+</sup> T cell, CD56<sup>+</sup> NK cell, and CD19<sup>+</sup> B cell fractions, and each cell fraction and all PBMCs were encapsulated into droplets. The ratio of vector-positive cells was determined by single cell-based digital droplet PCR (sc-ddPCR). Data were pooled from three independent experiments for each patient. (C) Bone marrow samples after lysis of red blood cells were also sorted and analyzed for the presence of the vector  $\psi$  sequence (whole bone marrow cells, CD34<sup>+</sup> cells). For each sample, sc-ddPCR was conducted in triplicate.

cell fractions of patients' PB and BM samples. The results in both patients demonstrated the selective potential of ADA-positive cells over non-transduced cells in the T cell population. Pt2 received T cell-mediated gene therapy with the  $\gamma$ -retrovirus vector LASN prior to SCGT,<sup>27</sup> which could potentially explain the slightly lower levels of vector integration in T cells, as our primers and probe could not detect the LASN sequence. Meanwhile, lower ratios of vector-positive cells were detected in other cell fractions from PB and BM.

Remarkably, a small number of gene-transduced cells remained in the BM CD34<sup>+</sup> cell population, which suggests that the circulating vector-positive

cells in our patients are derived from the small population of "stem cells" in BM or from the differentiated precursors downstream of the HSCs. This also indicated that even in gene therapy for SCID, securing "space" in the BM niche was necessary for engineered HSCs to engraft and differentiate into multiple lineages.

Based on this strategy, we established a new method for the absolute quantification of cells expressing the target gene. This novel system enables the direct detection of a target gene in a single cell without the extraction and amplification of genomic DNA. In establishing the strategy, we had some difficulties to overcome because the entire process from cell lysis to PCR amplification should be conducted within droplets. Inhibitors released from human blood cells such as lactoferrin<sup>26</sup> can inhibit direct PCR, and the target gene had to be amplified in the presence of these undesirable substances from lysed cells. Encapsulation of a single cell is another key factor for an accurate evaluation, because multi-cell encapsulation may lead to underestimation of the values. Increasing the PCR polymerase concentration and applying a low number of cells (2,000 cells) can provide precise amplification of the signal and make detailed analysis possible, even in small-scale cell samples.

The sc-ddPCR method enabled the detailed mapping of gene-transduced cells and revealed their complicated distribution in the specific

Calculating the tVCN is also important in assessing the risk of insertional oncogenesis due to vector integration,<sup>28–30</sup> because it has been proposed that vector integration at a few copies per cell may reduce the number of potential hits.<sup>31</sup> Using the sc-ddPCR system, we calculated the tVCNs in the treated patients and revealed that the transduced cells exhibited different levels of vector integration according to the lymphocyte lineage. In the experiments using K562 cells with various copy numbers (one to five copies) for evaluating this system, although spiked samples with one-copy cells had a coefficient of variation (CV) of more than 0.1, the calculated values ranged from 0.7 to 1.4, which could be determined as "1," and we concluded that the calculated values reflected the actual copy number.

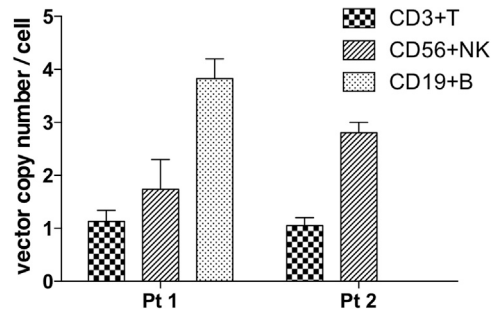


**Figure 5. Difference in Vector Copy Numbers in Gene-Transduced Cells between T Cell and Other Hematopoietic Lineages**

Vector copy numbers (VCNs) in gene-transduced cells (tVCNs) were calculated for CD3<sup>+</sup> T cells, CD19<sup>+</sup> B cells, and CD56<sup>+</sup> NK cells. The transduced cells displayed greater VCNs in B and NK cells compared to the value of approximately 1 in T cells (two independent experiments for each patient).

Recently, ddPCR enabled the assessment of gene expression profiles within a single cell by performing the RT reaction inside droplets.<sup>32</sup> In combination with RT, sc-ddPCR has the potential to detect transcription-active cells in the target population, and the difference in ratios between the vector-positive and transcription-active cells theoretically denotes “transcriptional suppression” in gene-transduced cells.

Overall, our novel system clarified vector integration in a single cell without any complex procedures, such as genome extraction and amplification, and single cell-based gene tracing allowed us to comprehensively analyze the engraftment of vector-transduced cells at the genetic level. Detailed information regarding the distribution of transduced cells in gene therapy-treated patients can be strongly advantageous for determining treatment strategies including conditioning therapy in SCGT clinical trials.

## MATERIALS AND METHODS

### Generation of K562 Cells Carrying the GCsapM-ADA-Internal Ribosome Entry Site EGFP Retroviral Vector

The original Molony murine leukemia virus (MoMLV)-based  $\gamma$ -retroviral vector GCsapM-ADA was described previously.<sup>33</sup> A fragment of the internal ribosome entry site (IRES) and EGFP cDNA was incorporated downstream of ADA cDNA (GCsapM-ADA-IE). Virus supernatant was prepared by transfecting the 293 gpg packaging cell line<sup>34</sup> with the resultant vector plasmid using the calcium phosphate transfection method and was used to transduce K562 cells. After cloning by limiting dilution, genomic DNA was extracted from each clone, and VCNs were determined using the QX200 ddPCR system (Bio-Rad Laboratories) with primers and probes for vector packaging signals ( $\psi$ ) and the internal reference gene *RPP30*.

### Patients

The patients’ characteristics and detailed information about the clinical trial were previously described.<sup>18</sup> In brief, Pt1 and Pt2 devel-

**Table 2. Vector Copy Numbers Limited to Transduced Cells in the Peripheral Blood and Bone Marrow Samples from Gene Therapy-Treated Patients**

	Peripheral Blood (Third Sample)			Bone Marrow		
	T Cell	B Cell	NK Cell	Whole	CD34 <sup>+</sup>	CD19 <sup>+</sup>
Patient 1						
VCN in gDNA (aVCN)	1.34	0.84	0.16	0.06	ND <sup>b</sup>	0.04
Ratio by sc-ddPCR	1.00 <sup>a</sup>	0.20	0.71	0.049	0.027	0.011
VCN/cell (tVCN)	1.34	4.2	2.3	1.2	ND	3.5
Patient 2						
VCN in gDNA (aVCN)	0.97	ND <sup>b</sup>	0.21	0.03	ND	0.03
Ratio by sc-ddPCR	0.82	0.10	0.08	0.07	ND	0.01
VCN/cell (tVCN)	1.2	ND	2.61	0.4	ND	3.0

VCN, average VCN in the extracted genomic DNA; ND, not detected; tVCN, VCN in the fraction of transduced cells.

<sup>a</sup>The number of signals for vector  $\psi$  was slightly higher than that for *RPP30*. The actual ratio of vector  $\psi$  to *RPP30* was 1.006 (100.6%).

<sup>b</sup>The aVCN measured in genomic DNA was lower than 0.005, and we could not calculate the tVCN. Representative data are shown.

oped clinical symptoms at 15 days and 8 months after birth, respectively, and they were treated with SCGT at the ages of 4.7 and 13.0 years, respectively. PEG-ADA treatment was withdrawn, and no cytoreductive therapy was administered before SCGT in either patient.

### Separation of Cell Subsets from PB and BM

Mononuclear cells were separated from the PB samples of both patients via density gradient centrifugation using Ficoll-Hypaque. Nuclear cells were collected from BM samples via erythrocyte lysis. Each immune phenotype subset was isolated by FACS using fluorescent-labeled antibodies (FACSaria II; BD Biosciences). The following monoclonal antibodies were used for positive selection: anti-CD3 (T cells), anti-CD19 (B cells), and anti-CD56 (NK cells).

### Design of Primers and Probes for Fluorescent PCR

The following primers and probes were used for detecting the retrovirus packaging signal: retrovirus  $\psi$  forward, 5'-gcaacctatctgtctgtccg-3'; retrovirus  $\psi$  reverse, 5'-gggccagagatacagag c-3'; retrovirus  $\psi$  probe, 5'-/FAM/tgcgctgc/ZEN/gtctgtactagtag/3IABkFQ/-3'; *RPP30* forward, 5'-tccaggaggagaattga tg-3'; *RPP30* reverse, 5'-atggctcctcag gaaa tg-3'; and *RPP30* probe, 5'-/HEX/tccctagg/ZEN/tggcctgagcag/3IABkFQ/-3'.

### sc-ddPCR

The PCR reaction mixture consisted of a 20- $\mu$ L solution containing 7.50  $\mu$ L ddPCR supermix, the probe at a concentration of 0.5 or 1.0  $\mu$ M, and 0.5  $\mu$ M primers for the target  $\psi$  and *RPP30*. 4  $\mu$ L KAPA2G Hot Start DNA polymerase (KAPA Biosystems), 2.80  $\mu$ L KAPA2G Hot Start buffer and enhancer, and SDS (0.015% final) were additionally applied to the mix, as described in Table S1. Sample cells were directly added, and droplets were generated using the Bio-Rad QX200 system following the manufacturer’s instructions. The

reactions were transferred to a 96-well plate for the PCR protocol using a C1000 Thermal Cycler (Bio-Rad). The thermal cycling program included the cell lysis step at 85°C for 60 min, initial denaturation at 95°C for 3 min, and 42 cycles of melting at 94°C for 30 s, annealing at 60°C for 60 s, and elongation at 72°C for 60 s. After the additional extension at 72°C for 10 min was completed, the 96-well plate was transferred to a QX200 Droplet Reader (Bio-Rad) and analyzed for the number of fluorescent-positive droplets. Detailed information about the composition of the reaction and PCR program is described in the [Supplemental Information](#).

The ratio of vector-positive cells was calculated as follows:

$$\text{Ratio of vector-positive cells} = \frac{(\text{number of vector positive droplets})}{(\text{number of } RPP30\text{-positive droplets})}$$

#### Genomic DNA Extraction and Conventional ddPCR

Genomic DNA was extracted from sorted cell subsets using a DNeasy Blood and Tissue Kit (QIAGEN) and then analyzed for vector  $\psi$  and *RPP30* copy numbers using multiplex ddPCR with standard procedures. For K562 cell samples spiked with one-copy K562-AE cells, the vector index was calculated as follows:

$$\text{Vector index} = \frac{(2 \times \text{number of vector-positive droplets})}{(\text{number of } RPP30\text{-positive droplets})}$$

An index of 1 indicated that all cells contained the provirus sequence, meaning that each cell had two copies of *RPP30* and one copy of vector  $\psi$ . The aVCN was calculated using genomic DNA extracted from patients' samples as follows:

$$\text{aVCN}(\text{VCNs/cell}) = \frac{(\text{number of vector-positive droplets})}{(0.5 \times \text{number of } RPP30\text{-positive droplets})}$$

#### Calculation of VCNs in Vector-Transduced Cells

tVCNs were determined on the basis of the ratios of gene-transduced cells and aVCNs, calculated using sc-ddPCR and a conventional ddPCR, respectively. The tVCN in each cell was calculated as follows:

$$\text{tVCN} = \text{aVCN}/(\text{ratio of vector-positive droplets}).$$

#### Study Approval

All study protocols involving the participation of patients were approved by the ethics committees at the National Center for Child Health and Development (NCCHD). PB and BM samples were obtained from both patients after written informed consent was obtained from the patients' parents, in line with standard ethical procedures.

#### SUPPLEMENTAL INFORMATION

Supplemental Information includes three figures and four tables and can be found with this article online at <http://dx.doi.org/10.1016/j.omtm.2017.05.005>.

#### AUTHOR CONTRIBUTIONS

Y.I. and T.U. designed and performed the experiments, analyzed data, and wrote the paper. T.M., N.W., and S.T. performed the experiments. T.K., M.Y., and T.A. provided technical support and conceptual advice. The entire process outlined in this paper was conducted by M.O.

#### CONFLICTS OF INTEREST

The authors have no conflicts of interest to disclose in relation to this article.

#### ACKNOWLEDGMENTS

The manuscript was proofed and edited by Emma Barber (Education for Clinical Research, NCCHD). We thank both patients and their families for their cooperation. We are also grateful to the medical staff who cared for the patients. We thank the laboratory staff at the NCCHD Department of Human Genetics for excellent support. We also thank Drs. Eiichiro Tamura, Fumihito Goto, and Yumiko Nakazawa for appropriate clinical and technical support. This work was supported by grants from the Japan Agency for Medical Research and Development and the NCCHD (to M.O.).

#### REFERENCES

- Bordignon, C., Notarangelo, L.D., Nobili, N., Ferrari, G., Casorati, G., Panina, P., Mazzolari, E., Maggioni, D., Rossi, C., Servida, P., et al. (1995). Gene therapy in peripheral blood lymphocytes and bone marrow for ADA- immunodeficient patients. *Science* 270, 470–475.
- Kohn, D.B., Weinberg, K.I., Nolte, J.A., Heiss, L.N., Lenarsky, C., Crooks, G.M., Hanley, M.E., Annett, G., Brooks, J.S., el-Khoureyi, A., et al. (1995). Engraftment of gene-modified umbilical cord blood cells in neonates with adenosine deaminase deficiency. *Nat. Med.* 1, 1017–1023.
- Malech, H.L., Maples, P.B., Whiting-Theobald, N., Linton, G.F., Sekhsaria, S., Vowells, S.J., Li, F., Miller, J.A., DeCarlo, E., Holland, S.M., et al. (1997). Prolonged production of NADPH oxidase-corrected granulocytes after gene therapy of chronic granulomatous disease. *Proc. Natl. Acad. Sci. USA* 94, 12133–12138.
- Kohn, D.B., Hershfield, M.S., Carbonaro, D., Shigeoka, A., Brooks, J., Smogorzewska, E.M., Barsky, L.W., Chan, R., Burotto, F., Annett, G., et al. (1998). T lymphocytes with a normal ADA gene accumulate after transplantation of transduced autologous umbilical cord blood CD34+ cells in ADA-deficient SCID neonates. *Nat. Med.* 4, 775–780.
- Cavazzana-Calvo, M., Hacein-Bey, S., de Saint Basile, G., Gross, F., Yvon, E., Nussbaum, P., Selz, F., Hue, C., Certain, S., Casanova, J.L., et al. (2000). Gene therapy of human severe combined immunodeficiency (SCID)-X1 disease. *Science* 288, 669–672.
- Aiuti, A., Slavina, S., Aker, M., Ficara, F., Deola, S., Mortellaro, A., Morecki, S., Andolfi, G., Tabucchi, A., Carlucci, F., et al. (2002). Correction of ADA-SCID by stem cell gene therapy combined with nonmyeloablative conditioning. *Science* 296, 2410–2413.
- Gaspar, H.B., Parsley, K.L., Howe, S., King, D., Gilmour, K.C., Sinclair, J., Brouns, G., Schmidt, M., Von Kalle, C., Barington, T., et al. (2004). Gene therapy of X-linked severe combined immunodeficiency by use of a pseudotyped gammaretroviral vector. *Lancet* 364, 2181–2187.
- Gaspar, H.B., Björkregren, E., Parsley, K., Gilmour, K.C., King, D., Sinclair, J., Zhang, F., Giannakopoulos, A., Adams, S., Fairbanks, L.D., et al. (2006). Successful reconstitution of immunity in ADA-SCID by stem cell gene therapy following cessation of PEG-ADA and use of mild preconditioning. *Mol. Ther.* 14, 505–513.
- Aiuti, A., Cattaneo, F., Galimberti, S., Benninghoff, U., Cassani, B., Callegaro, L., Scaramuzza, S., Andolfi, G., Mirolo, M., Brigida, I., et al. (2009). Gene therapy for immunodeficiency due to adenosine deaminase deficiency. *N. Engl. J. Med.* 360, 447–458.

10. Hacein-Bey-Abina, S., Hauer, J., Lim, A., Picard, C., Wang, G.P., Berry, C.C., Martinache, C., Rieux-Laucat, F., Latour, S., Belohradsky, B.H., et al. (2010). Efficacy of gene therapy for X-linked severe combined immunodeficiency. *N. Engl. J. Med.* 363, 355–364.
11. Gaspar, H.B., Cooray, S., Gilmour, K.C., Parsley, K.L., Adams, S., Howe, S.J., Al Ghonaium, A., Bayford, J., Brown, L., Davies, E.G., et al. (2011). Long-term persistence of a polyclonal T cell repertoire after gene therapy for X-linked severe combined immunodeficiency. *Sci. Transl. Med.* 3, 97ra79.
12. Gaspar, H.B., Cooray, S., Gilmour, K.C., Parsley, K.L., Zhang, F., Adams, S., Björkregren, E., Bayford, J., Brown, L., Davies, E.G., et al. (2011). Hematopoietic stem cell gene therapy for adenosine deaminase-deficient severe combined immunodeficiency leads to long-term immunological recovery and metabolic correction. *Sci. Transl. Med.* 3, 97ra80.
13. Macaulay, I.C., and Voet, T. (2014). Single cell genomics: advances and future perspectives. *PLoS Genet.* 10, e1004126.
14. Hershfield, M.S. (1998). Adenosine deaminase deficiency: clinical expression, molecular basis, and therapy. *Semin. Hematol.* 35, 291–298.
15. Hershfield, M.S., Buckley, R.H., Greenberg, M.L., Melton, A.L., Schiff, R., Hatem, C., Kurtzberg, J., Markert, M.L., Kobayashi, R.H., Kobayashi, A.L., et al. (1987). Treatment of adenosine deaminase deficiency with polyethylene glycol-modified adenosine deaminase. *N. Engl. J. Med.* 316, 589–596.
16. Chan, B., Wara, D., Bastian, J., Hershfield, M.S., Bohnsack, J., Azen, C.G., Parkman, R., Weinberg, K., and Kohn, D.B. (2005). Long-term efficacy of enzyme replacement therapy for adenosine deaminase (ADA)-deficient severe combined immunodeficiency (SCID). *Clin. Immunol.* 117, 133–143.
17. Candotti, F., Shaw, K.L., Muul, L., Carbonaro, D., Sokolic, R., Choi, C., Schurman, S.H., Garabedian, E., Kesslerwan, C., Jagadeesh, G.J., et al. (2012). Gene therapy for adenosine deaminase-deficient severe combined immune deficiency: clinical comparison of retroviral vectors and treatment plans. *Blood* 120, 3635–3646.
18. Otsu, M., Yamada, M., Nakajima, S., Kida, M., Maeyama, Y., Hatano, N., Toita, N., Takezaki, S., Okura, Y., Kobayashi, R., et al. (2015). Outcomes in two Japanese adenosine deaminase-deficiency patients treated by stem cell gene therapy with no cytoreductive conditioning. *J. Clin. Immunol.* 35, 384–398.
19. Aiuti, A., Biasco, L., Scaramuzza, S., Ferrua, F., Cicalese, M.P., Baricordi, C., Dionisio, F., Calabria, A., Giannelli, S., Castiello, M.C., et al. (2013). Lentiviral hematopoietic stem cell gene therapy in patients with Wiskott-Aldrich syndrome. *Science* 341, 1233151.
20. Nakazawa, Y., Kawai, T., Uchiyama, T., Goto, F., Watanabe, N., Maekawa, T., Ishiguro, A., Okuyama, T., Otsu, M., Yamada, M., et al. (2015). Effects of enzyme replacement therapy on immune function in ADA deficiency patient. *Clin. Immunol.* 161, 391–393.
21. Villella, A.D., Yao, J., Getty, R.R., Juliar, B.E., Yiannoutsos, C., Hartwell, J.R., Cai, S., Sadat, M.A., Cornetta, K., Williams, D.A., and Pollok, K.E. (2005). Real-time PCR: an effective tool for measuring transduction efficiency in human hematopoietic progenitor cells. *Mol. Ther.* 11, 483–491.
22. Charrier, S., Ferrand, M., Zerbato, M., Précigout, G., Viornery, A., Bucher-Laurent, S., Benkhalifa-Ziyyat, S., Merten, O.W., Perea, J., and Galy, A. (2011). Quantification of lentiviral vector copy numbers in individual hematopoietic colony-forming cells shows vector dose-dependent effects on the frequency and level of transduction. *Gene Ther.* 18, 479–487.
23. Hindson, B.J., Ness, K.D., Masquelier, D.A., Belgrader, P., Heredia, N.J., Makarewicz, A.J., Bright, I.J., Lucero, M.Y., Hiddessen, A.L., Legler, T.C., et al. (2011). High-throughput droplet digital PCR system for absolute quantitation of DNA copy number. *Anal. Chem.* 83, 8604–8610.
24. Moser, D.A., Braga, L., Raso, A., Zacchigna, S., Giacca, M., and Simon, P. (2014). Transgene detection by digital droplet PCR. *PLoS ONE* 9, e111781.
25. Abyzov, A., Mariani, J., Palejev, D., Zhang, Y., Haney, M.S., Tomasini, L., Ferrandino, A.F., Rosenberg Belmaker, L.A., Szekely, A., Wilson, M., et al. (2012). Somatic copy number mosaicism in human skin revealed by induced pluripotent stem cells. *Nature* 492, 438–442.
26. Al-Soud, W.A., and Rådström, P. (2001). Purification and characterization of PCR-inhibitory components in blood cells. *J. Clin. Microbiol.* 39, 485–493.
27. Onodera, M., Ariga, T., Kawamura, N., Kobayashi, I., Ohtsu, M., Yamada, M., Tame, A., Furuta, H., Okano, M., Matsumoto, S., et al. (1998). Successful peripheral T-lymphocyte-directed gene transfer for a patient with severe combined immune deficiency caused by adenosine deaminase deficiency. *Blood* 91, 30–36.
28. Hacein-Bey-Abina, S., Garrigue, A., Wang, G.P., Soulier, J., Lim, A., Morillon, E., Clappier, E., Caccavelli, L., Delabesse, E., Beldjord, K., et al. (2008). Insertional oncogenesis in 4 patients after retrovirus-mediated gene therapy of SCID-X1. *J. Clin. Invest.* 118, 3132–3142.
29. Howe, S.J., Mansour, M.R., Schwarzwald, K., Bartholomae, C., Hubank, M., Kempski, H., Brugman, M.H., Pike-Overzet, K., Chatters, S.J., de Ridder, D., et al. (2008). Insertional mutagenesis combined with acquired somatic mutations causes leukemogenesis following gene therapy of SCID-X1 patients. *J. Clin. Invest.* 118, 3143–3150.
30. Braun, C.J., Boztug, K., Paruzynski, A., Witzel, M., Schwarzer, A., Rothe, M., Modlich, U., Beier, R., Göhring, G., Steinemann, D., et al. (2014). Gene therapy for Wiskott-Aldrich syndrome—long-term efficacy and genotoxicity. *Sci. Transl. Med.* 6, 227ra33.
31. Sadelain, M. (2004). Insertional oncogenesis in gene therapy: how much of a risk? *Gene Ther.* 11, 569–573.
32. Klein, A.M., Mazutis, L., Akartuna, I., Tallapragada, N., Veres, A., Li, V., Peshkin, L., Weitz, D.A., and Kirschner, M.W. (2015). Droplet barcoding for single-cell transcriptomics applied to embryonic stem cells. *Cell* 161, 1187–1201.
33. Onodera, M., Nelson, D.M., Yachie, A., Jagadeesh, G.J., Bunnell, B.A., Morgan, R.A., and Blaese, R.M. (1998). Development of improved adenosine deaminase retroviral vectors. *J. Virol.* 72, 1769–1774.
34. Ory, D.S., Neugeboren, B.A., and Mulligan, R.C. (1996). A stable human-derived packaging cell line for production of high titer retrovirus/vesicular stomatitis virus G pseudotypes. *Proc. Natl. Acad. Sci. USA* 93, 11400–11406.